THE SUBURBAN ENERGY BALANCE IN MIAMI, FLORIDA

BY
T. NEWTON[1], T.R. OKE[1], C.S.B. GRIMMOND[2] AND M. ROTH[3]

[1]Department of Geography, University of British Columbia, Vancouver, Canada
[2]Department of Geography, King's College London, UK
[3]Department of Geography, National University of Singapore, Singapore

Newton, T., Oke, T.R., Grimmond, C.S.B. and Roth, M., 2007: The suburban energy balance in Miami, Florida. *Geogr. Ann.*, 89 A (4): 331–347.

ABSTRACT. Summertime measurements of local scale energy balance of a suburban site in west Miami, Florida, in 1995 are presented. All of the radiation and turbulent heat fluxes were measured directly. In addition several derived surface characteristics are calculated including the albedo, radiation temperature, emissivity, aerodynamic and canopy resistances, Bowen's ratio, Priestley–Taylor and McNaughton–Jarvis coefficients. The results are used to test parameterizations to calculate several heat fluxes. Most radiation fluxes can be calculated with simple schemes in cloudless conditions but the spatial and temporal variability of cloud degrades results greatly. This highlights the value of observing incoming solar radiation since it can form an excellent surrogate for daytime net all-wave radiation in all sky conditions. The heat flux results for this warm, wet subtropical site demonstrate similarities with those from similarly developed locations in temperate climates. Interestingly this finding includes the fraction of energy used in evaporation. It is thought that this may be related to the relatively large heat storage in Miami which may reflect the presence of wet soils and free-standing water, the persistently low vapor pressure deficits (7–14 hPa) typical of this humid climate and the relatively poor coupling between the surface and the whole planetary boundary layer due to relatively low surface roughness.

Key words: urban energy balance, radiation, evaporation, subtropical

Introduction

The surface energy balance is forced by the exchange of radiation between the Sun, the atmosphere, and the surface. The surface radiation budget consists of five terms, which can be separated into three categories based on wavelength. The net all-wave radiative flux density (Q^*) is equal to the sum of the net shortwave flux density ($K^* = K\downarrow - K\uparrow$) and the net longwave flux density ($L^* = L\downarrow - L\uparrow$). Shortwave fluxes refer to radiation in wavelengths ranging from 0.15 to 3.0 μm, and longwave to that between 3 and 100 μm (Oke 1987, p.11). The surface radiation budget therefore is:

$$Q^* = K\downarrow - K\uparrow + L\downarrow - L\uparrow \qquad (\mathrm{W\ m^{-2}}) \qquad (1)$$

Surface control is exerted by the surface albedo (α, which is the spectral reflectivity integrated over the shortwave band, i.e. $K\uparrow / K\downarrow$); the surface emissivity (ε_o) and the apparent surface radiant temperature (T_o, which from the Stefan-Boltzmann equation is $(L\uparrow / \varepsilon_o\, \sigma)^{0.25}$, where σ is Stefan's constant $= 5.67 \times 10^{-8}$ W m^{-2} K^{-4}. For most natural surfaces the net radiation is partitioned into the conductive exchange between the surface and the underlying substrate (Q_G) and the turbulent fluxes of sensible heat (Q_H) and latent heat (Q_E) between the surface and the overlying atmospheric boundary layer, so that:

$$Q^* = Q_G + Q_H + Q_E \qquad (\mathrm{W\ m^{-2}}) \qquad (2)$$

In the case of urbanized systems the equivalent flux of heat across the top of a layer due to heat storage change (ΔQ_S) in the volume is more appropriate than that across the interface, (see Oke 1988, p. 472), and the left-hand side of Equation 2 is supplemented by an anthropogenic flux contributed by the waste heat released due to human activities involving vehicles, space heating/cooling and industrial processing (Q_F). In the present study Q_F was not evaluated but is likely to be relatively small (say <20 W m^{-1}; e.g. Sailor and Lu 2004). The surface energy balance here is evaluated as:

$$Q^* = \Delta Q_S + Q_H + Q_E \qquad (\mathrm{W\ m^{-2}}) \qquad (3)$$

Very few previous urban energy balance studies

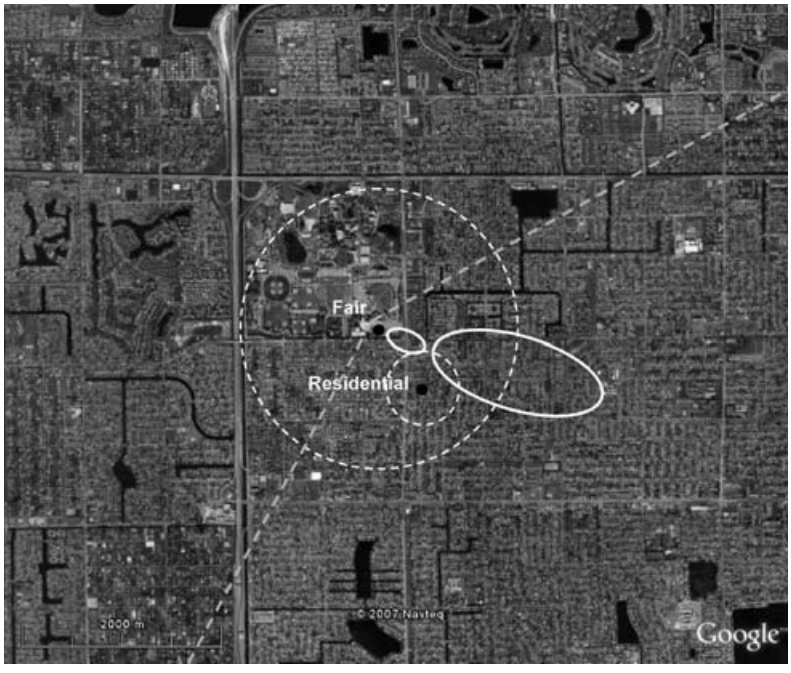

Fig. 1. Aerial photograph of the Miami suburban site including the location of the Fair and Residential towers, their radiation (circular) and turbulent (elliptical) source areas and the accepted sector for flow (60 to 210 degrees, dash-dot lines). The larger turbulent footprint is a stable (end of night) case and the smaller one is an unstable (afternoon) case.
Source: Google Earth©

have been conducted in subtropical or tropical climate regions. The first and most studied is Mexico City in a tropical highland climate (Oke *et al.* 1992, 1999; Barradas *et al.* 1999; Tejeda-Martinez and Jauregui 2005). Three dry-climate cities have also been investigated: Tucson, Arizona, in a subtropical desert climate (Grimmond and Oke 1995, 1999a); and Mexacali (Garcia-Cueto *et al.* 2003) and Ouagadougou, Burkina Faso, in a subtropical steppe climate (Offerle *et al.* 2005).

The aim of this study is to consider the case of the energy balance climate of a suburb of Miami, Florida, characterized by a high water table, drainage canals and many water storage ponds, and exposed to warm and humid air advected by the persistent sea breezes and the Trade winds. These properties give the chance to study the role of evaporation in the energy balance partitioning of a North American suburb. An appropriate framework to discuss controls on evaporation is the Penman–Monteith equation:

$$Q_E = [\, s\,(Q^* - \Delta Q_S) + (C_a\,V)\,/\,r_{aH}\,]\,/\,[\, s + \gamma\,(\,1 + r_c\,/\,r_{aH}\,)\,] \quad (\mathrm{W\ m^{-2}}) \qquad (4)$$

where s is the slope of the saturation vapour pressure versus temperature relation, C_a is the heat capacity of air, V is the vapour pressure deficit, γ is the psychrometric 'constant', r_{aH} is the aerodynamic resistance for heat transfer and r_c is the surface resistance. Miami provides an environment that might be expected to favour evaporation: strong radiative forcing, abundant water availability, warm air and good airflow. However, the relatively low vapour pressure deficit is likely to be less favourable.

Methods

Study site and area

The southeastern edge of the Florida peninsula is essentially a north–south orientated strip of land about 15 to 25 km wide and 150 km long, with Miami situated approximately 50 km north of the southern end. This strip is bounded by the swamps of the Everglades to the south and west, and by the Atlantic Ocean to the east. The greater Miami area is flat with no natural topographic features over 2 m in elevation. The natural vegetation is marsh grasses in marine areas (adjacent to swamps and canals), and in less wet regions, palm and ficus trees, and leafy fruit trees and bushes. South Florida has a hot-dry climate in winter and a hot-wet climate in summer.

Table 1. (a) Plan area fractions of surface types within a circle of radius 1 km around the Fair and Residential site and (b) their instrumentation

(a) Surface types

Site	Buildings	Impervious	Unmanaged	Trees	Grass	Water
Residential	0.33	0.20	0.04	0.08	0.34	0.02
Fair	0.29	0.29	0.03	0.06	0.28	0.04

(b) Instrumentation

Instrument	Variable	Height (m)
Residential		
Pyranometer (Eppley)	$K\uparrow$	10
Pyrgeometer (Eppley)	$L\uparrow$	10
Net radiometer (REBS Q6)	Q^*	10
Fair		
Pyranometer (Eppley)	$K\downarrow$	2.5
Pyrgeometer (Eppley)	$L\downarrow$	2.5
Net radiometer (REBS Q6)	Q*	40.6
3-D sonic anemometer (Gill)	*u', v', w', T'*	40.8
1-D sonic anemometer (CSI), fine-wire thermocouple (CA27)	*w', T'*	40.8
Anemometer and vane (RM Young)	*u*, wind direction (*dir*)	41
Krypton hygrometer (CSI, KH20)	*q'*	40.8
T/RH probe (Vaisala HMPC)	*T, RH*	40.7
Barometer	atmospheric pressure	2
Tipping bucket raingauge	precipitation	0.5

Two sites were established in western Miami (25°44'N, 80°22'W) (Table 1, Fig. 1). The general area is mainly single-storey residences with gardens and both garden and street trees. Analysis of aerial photographs and foot surveys gave the average plan fractions of land cover (Table 1) and suggests a mean building height of 6.9 m, a mean element spacing of about 17 m, a roughness element plan density of 0.41, a surface roughness length of 0.46 m, and a roughness sublayer (or blending) height of about 20 m (Grimmond and Oke 1999b). One site, called 'Fair', is a county fairground located in the southeastern corner of Tamiami Park. The immediate surroundings comprise a mixture of treed, grassed and paved surfaces, with a few buildings. These properties differ from those of the general suburban area of interest. However, the site was only used to measure incoming radiation fluxes ($K\downarrow$, $L\downarrow$,.which are unaffected by the surface characteristics, and the turbulent fluxes (Q_H, Q_E) whose sensors were mounted at about 40 m. Turbulent signals originate from source areas upstream of the site depending on the wind direction and atmospheric stability. There is about 10 km of suburban fetch upstream of the tower in this sector and the sites are approximately 13 km inland.

The other site, called 'Residential', is 0.7 km southeast of the Fair site in the backyard of a single-storey house in west Miami. The lot is grassed and occasionally irrigated with several leafy trees 2 to 8 m high. The three houses nearby have white stucco walls, and reddish-brown roofs (two have shingles and one has ceramic tiles) and each has a light-coloured metal garden shed. The site would fall into the **UCZ (urban climate zone)** class 5 of Oke (2004).

Instruments and their source areas

The instrumentation and height of exposure at the two sites is given in Table 1. The eddy covariance approach was used to measure directly the turbulent sensible and latent heat fluxes. The vertical wind velocity, air temperature, and humidity fluctuations were sampled at 5 Hz and covariances determined over 15-min periods. Flux corrections were made for oxygen absorption by the sensor (Tanner and Greene 1989) and air density (Webb *et al.* 1980). No corrections were made for frequency response or spatial separation of the sensors (see Grimmond and Oke (1995) for a discussion of implications). The 15 min data are averaged to 60 min for analysis.

The surface area 'seen' (their source areas, or

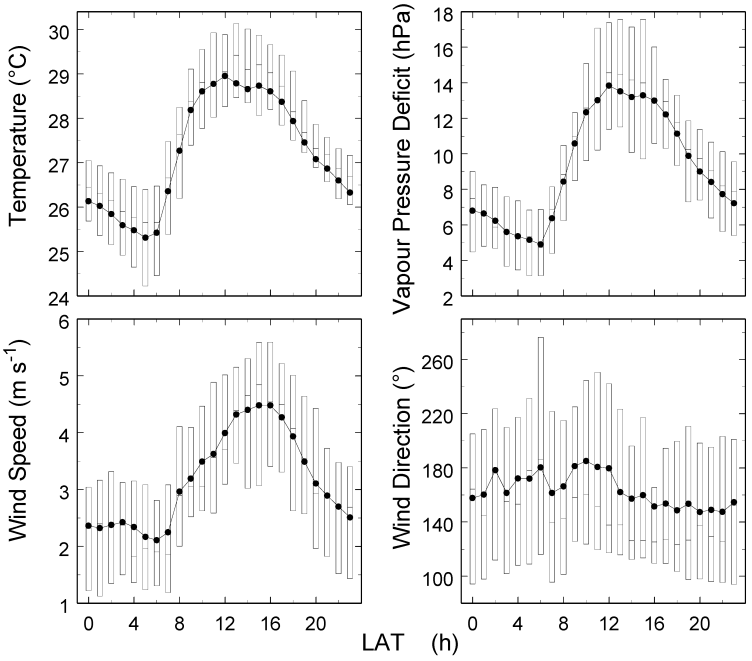

Fig. 2. Ensemble hourly averages of air temperature, vapour pressure deficit, wind speed, and wind direction at the 40 m level on the Fair tower for the 40-day observation period. The top of each boxplot corresponds to the 75th percentile for the hour, the horizontal line is the median, and the bottom is the 25th percentile

'footprints') by the downfacing radiation and turbulent flux sensors was calculated. The circular source areas for the upwelling radiative fluxes are calculated for the two sites using Schmid *et al.* (1991, p. 258, see Fig. 1). Turbulent source areas ('footprints') were derived from Schmid (1994). Because the sensors are mounted at 40 m, which is about twice the blending height, they give spatially representative fluxes of the suburban area as long as the flow is from the correct sector. Observations were filtered according to wind direction. Flow from directions not representative of the suburban region were discarded, as were those directions likely to be disturbed by wake effects generated by the tower or the mounting cross-arm or other sensors. The accepted range of wind directions is from 60° to 210° (Fig. 1). Examples of the elliptical footprints containing 50% of the measured flux are given in Fig. 1 for stable and unstable cases.

The heat storage change (ΔQ_S) values reported here are not directly measured. They are residuals from Equation 3 after having inserted measured values of the radiation and turbulent terms. They therefore suffer by accumulating the errors in the measured Q^*, Q_H and Q_E estimates. The lack of an absolute standard or a better method to evaluate ΔQ_S remains a significant limitation in urban energy balance climatology (Roberts *et al.* 2006).

Weather during the observation period

Weather conditions during the observation period (13 May, YD 133 to 21 June YD 172, 1995; **YD = year day**, i.e. YD 1 = 1 January) are characterized by an especially pronounced diurnal cycle (Fig. 2); days are generally sunny, mornings are clear, in the afternoon cloud and eventually thunderstorms develop. Air temperature and vapour pressure deficit show relatively little variation. Both show dips in the early afternoon associated with cumulus development and patchy thundershowers. The average air temperature was 27.2°C; this is 0.9°C warmer than the 1961–90 normal. Vapour pressure deficits were low, typically 5 to 14 hPa. Breezes, predominantly from the south and southeast, are present even at night, reaching about 4 m s^{-1} in the afternoon. Most precipitation was associated with short-lived synoptic or meso-scale troughs. On 19 of the 40 days rainfall exceeded 0.25 mm, 3 days more than normal.

Observed values

Radiation

The ensemble mean of the observed radiation budget components at the suburban Miami site describe relatively smooth curves both in cloudless and all-sky conditions (Fig. 3). As at temperate cli-

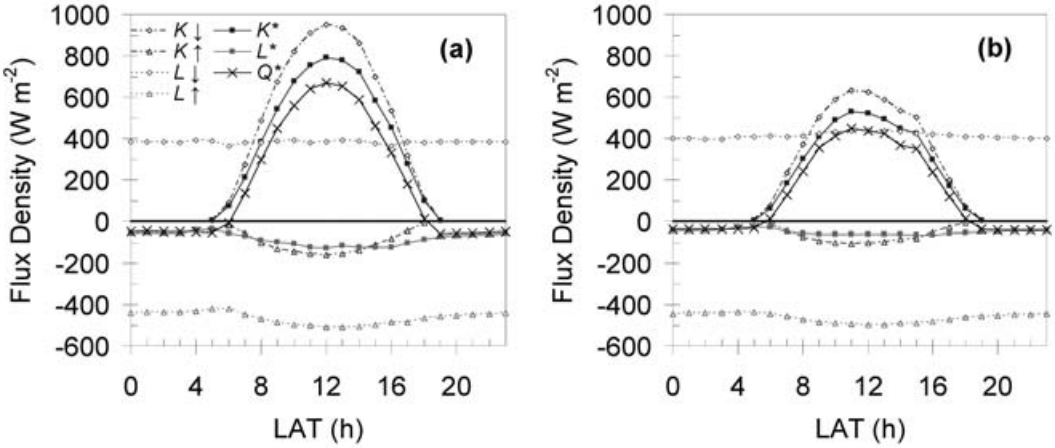

Fig. 3. Ensemble hourly averaged radiation flux densities measured over a 40-day period in 1995 (YD133–172) at the Residential site in (a) cloudless, and (b) all-sky conditions. (The sign convention for radiation is that all downward fluxes are positive, and all upward fluxes are negative)

mate urban and suburban sites, the overall form of the budget is very similar to that of many other natural land ecosystems (e.g. Davies and Idso 1979; Oke 1987; Monteith and Unsworth 1990; Bailey *et al.* 2000). There is little to identify the results as being from an urbanized site where the heterogeneous nature of both the polluted atmosphere and of the urban surface cover and geometry might perhaps be anticipated to lead to more erratic radiative flux behaviour or distinct flux partitioning. Naturally the absolute magnitude of the incoming solar flux is relatively large since the site is at latitude 26°N and the period is just prior to the summer solstice. Incoming longwave radiation is also large due to the warm and humid air masses. These larger inputs do produce a slightly larger daytime net all-wave radiation surplus than at other suburban sites in summertime but there is no reason to believe that the increase is not mirrored in nearby rural areas.

Cloud cover observations were obtained from Miami International Airport. Of the 855 hours of radiation observations, only 9% (77 hours) were with clear-sky conditions; the rest were classified as 'cloudy' if any cloud was present. This means the results reported as cloudless are sparse and possess less robust statistics. However, apart from the apparent 'dip' in the early afternoon inputs, the cloudless and all-sky results differ only in respect of their absolute magnitude.

Three assessments of Q^* are possible, given the instrument array: Q^*_{fair} from the 40 m radiometer at the Fair site; $Q^*_{residential}$ from the 10 m radiometer at the Residential site; and Q^*_{sum} the sum of the four separately observed fluxes, i.e. the downwelling fluxes at Fair and the upwelling ones at Residential. The three Q^* measurements agree quite closely throughout the day in cloudless conditions. With cloud the three measurements differed more, probably mainly due to the spatial variation of incoming fluxes induced by patchy cumulus. Given the differing surface cover $Q^*_{residential}$ is likely to be most representative of the suburban district despite the relatively small source area sampled.

The ensemble-averaged albedo (α) shows a relatively steady downward trend through the day (from about 0.20 to 0.14). The trend is not expected but other urbanized sites have shown other than the more standard U-shape versus time curve (e.g. Rouse and Bello (1979) in Hamilton, Ontario; Steyn and Oke (1980) in Vancouver). The trend could be the result of local effects such as shade or anomalous materials, or the $K\uparrow$ sensor not being sufficiently level. Restricting results to the midday period of greatest energy input (1000 to 1400 **local apparent time (LAT)** with solar zenith angles <35° and taking the ratio of the sum of the upwelling and downwelling solar fluxes, the mean observed albedo between 1000 and 1400 LAT is 0.168 with clear skies, and 0.164 under all-sky conditions. This albedo is consistent with the average value of 0.15 based on a survey of suburban experimental studies (Oke 1988) which is not contradicted by more recent suburban studies (e.g. Christen and Vogt 2004; Offerle *et al.* 2006). Indeed the Miami value would probably be higher if it were not for the standing water bodies.

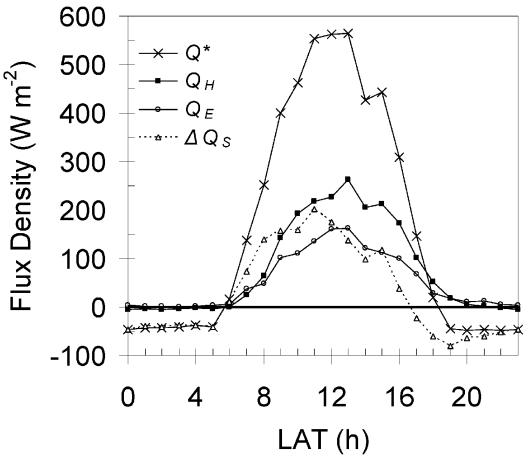

Fig. 4. Ensemble hourly averaged energy flux densities measured over a 40-day period in 1995 (YD133–172) at the Fair site. Note: the Q^* trace differs from that in Fig. 3 because only those hours adhering to the criteria for turbulent observations are used here. (The sign convention is that non-radiative terms directed away from the surface are positive)

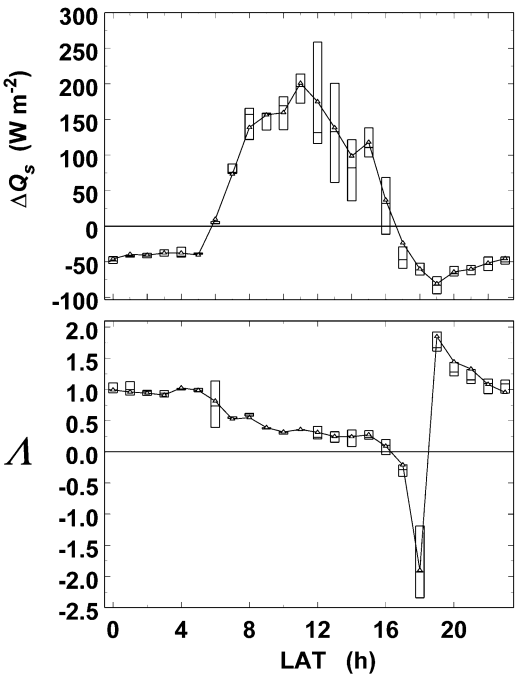

Fig. 5. Ensemble hourly averages of ΔQ_s and Λ (= $\Delta Q_s/Q^*$) over the entire observation period. The boxplot convention is as in Fig. 2

T_o values are calculated using $L\uparrow_{residential}$ and the Stefan–Boltzmann relation. A surface emissivity of 0.97 gives values that agree best with the independent measures of air temperature and the corresponding turbulent sensible heat flux. That is, the surface-air temperature lapse rate agrees in sign and approximate magnitude with the flux (see below). Under clear-sky conditions T_o peaks at 1300 LAT, whereas T_a does so between 1600 and 1700 LAT. Under cloudy conditions T_o and T_a are more in phase, peaking near solar noon due in part to the prolific cloud build-up by early afternoon. Given the subtropical radiation forcing, the daily range of ensemble average surface temperature is relatively small – about 14.5 K on clear days and only about 9.5 K in all-sky conditions. This is probably partly attributable to mixing by the brisk airflow but mostly to the high heat capacity of the wet ground and bodies of standing water.

Energy

The ensemble-average energy balance for all-sky conditions is given in Fig. 4. By day the largest flux is the convective transport of sensible heat (Q_H), second is the sensible heat storage (ΔQ_s) and the smallest fraction is used in evaporation (Q_E). The phase of the fluxes is different, with ΔQ_s peaking in the late morning, and Q_E and Q_H in the early afternoon. The main exchange at night has the net radiation drain almost totally matched by release of heat from storage. The turbulent fluxes are both small but in the afternoon and evening, up to about 2200 LAT, both turbulent fluxes are away from the surface. For the first three hours after sunset this is supported by a large release from storage. This daily balance looks similar to those in several other suburban sites in temperate climates (e.g. Grimmond and Oke 1999b, 2002).

Storage heat flux (ΔQ_s). The absolute values and temporal behaviour of ΔQ_s and the fraction of the net radiation involved in heat storage Λ (= $\Delta Q_s/Q^*$) in Miami (Fig. 5) are similar to those observed in other cities, and nearly identical to those recorded in the subtropical desert city of Tucson (Grimmond and Oke 1995). For both cities, ΔQ_s peaks at about 200 W m^{-2} shortly before solar noon, drops to its daily minimum near sunset, recovers somewhat by midnight, thereafter remaining fairly constant until sunrise. The main differences between the ΔQ_s of the two cities are that the negative nocturnal ΔQ_s values are larger in Tucson (–100 versus

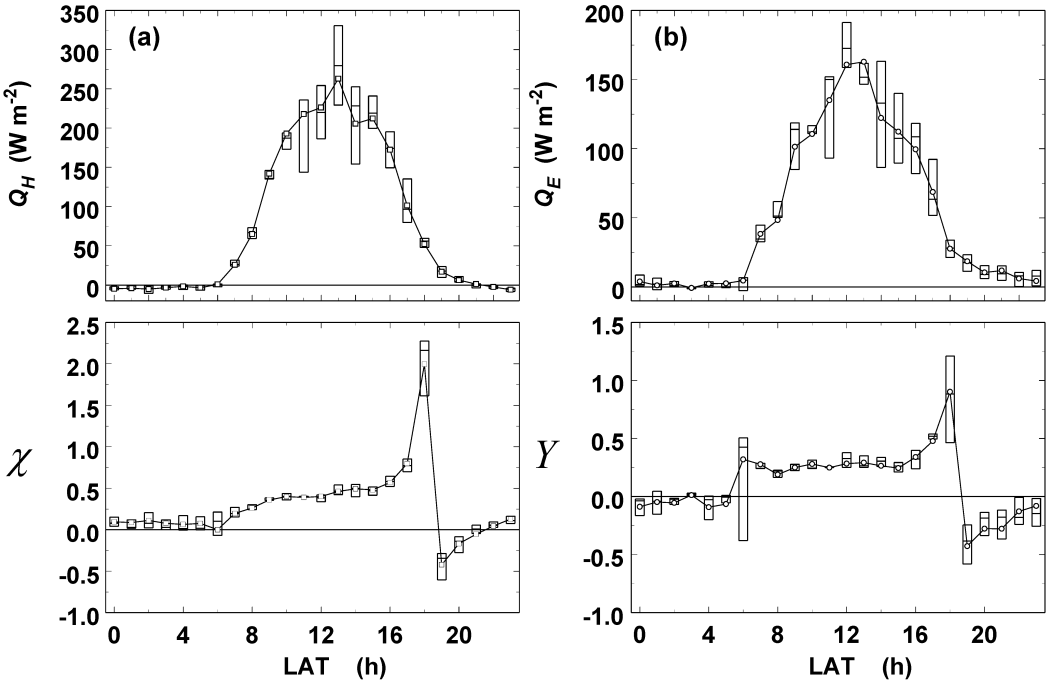

Fig. 6. Ensemble hourly averages of (a) Q_H and χ (Q_H/Q^*) and (b) Q_E and Y (= Q_E/Q^*) over the observation period. The boxplot convention is as in Fig. 2. Note the scale difference between (a) and (b)

–50 W m^{-2}), consistent with the greater Q^* loss in Tucson, and average daytime Λ is larger in Miami (0.30 versus 0.23) (Grimmond and Oke 1999a).

The diurnal variation of Λ in Miami is also essentially similar to that observed in suburban residential areas of Chicago, Los Angeles and Sacramento (Grimmond and Oke 1995). The steady daytime decrease from *c*. 0.5 near sunrise to zero at sunset is present in all cases (Fig. 5). The trend is due to the pattern of hysteresis between ΔQ_S and Q^*. Hysteresis is particularly pronounced in Miami and Chicago, compared to other cities (Grimmond and Oke 1999a). In essence the trend is the mirror-image of that for Q_H (Fig. 6a) reflecting the daily change in sensible heat sharing between conduction and convection, while the fraction used by evaporation remains fairly constant (Fig. 6b).

At night, in Chicago, Sacramento and Tucson, Λ has the fairly constant value of unity; i.e. the radiation loss is supplied almost entirely by removal of heat from storage. The same is largely true for Miami, although ΔQ_S is greater than Q^* for about three hours after sunset (Fig. 5). The 'excess' removal of stored sensible heat is partitioned into evaporation (Q_E), and for about two hours into nocturnal convection (Q_H). Similar post-sunset 'blips' in removal of heat from storage are evident for Chicago and Tucson, but they last for only an hour, not four. The abrupt nature of sunset at low latitudes may be involved.

The average daytime and all-day Λ in Miami are 0.30 and 0.18, respectively. They are near the upper end of the observed range of suburban values (Grimmond and Oke 1999a; Christen and Vogt 2004). Only at the Arcadia site in Los Angeles have slightly higher values been recorded: daytime 0.31 and all-day 0.21. It is not particularly surprising that heat storage plays a large role in the energy régime of Miami given the water present in the soil, vegetation, air, and canals and lakes which aid efficient absorption of heat and provide a large heat capacity.

Turbulent sensible heat flux (Q_H). The ensemble-mean turbulent sensible heat flux (Q_H) peak occurs about one hour after the maximum Q^* (Fig. 6a upper panel). As with T_0, the day-to-day variability of Q_H is greatest around midday and the afternoon and this is clearly related to the appearance of cloud (Figs 4 and 5). The flux does not turn negative until 2100 LAT, several hours after Q^*, and then remains negative until near sunrise. This behaviour is observed at most other sites where there is urban de-

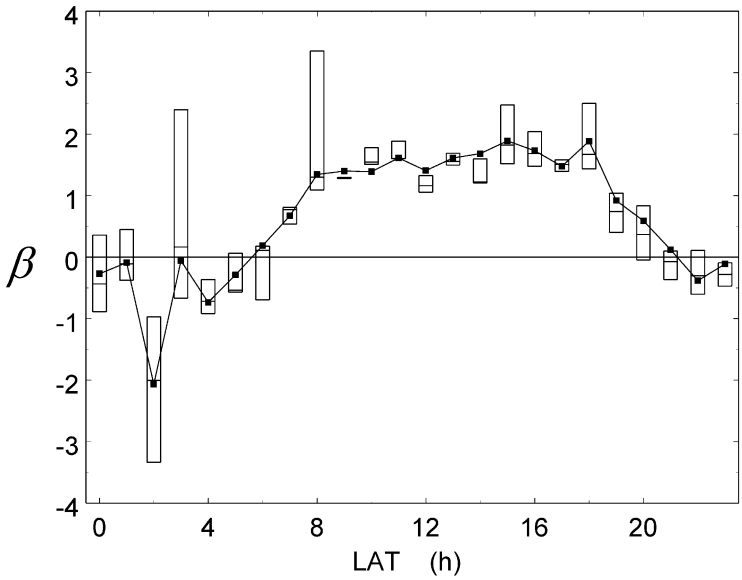

Fig. 7. Ensemble hourly averaged Bowen ratio (ß) over the observation period. The black squares are the averages of all data (the 0th through the 100th percentile) for each hour

velopment, with the length of delay tending to increase with the urban density (Oke 1988; Grimmond and Oke 2002; Christen and Vogt 2004).

The share of the net radiation going into Q_H ($\chi = Q_H/Q^*$) shows remarkably little day-to-day variability especially in the daytime (Fig. 6a), i.e. almost irrespective of weather conditions. This suggests a robust basis for parameterization. The upward trend of the χ curve through the daytime is part of a hysteresis pattern found at temperate suburban and urban sites. This is connected to the diurnal variation of static stability: increasing instability as the day progresses favours convection over conduction, hence sensible heat sharing favours ΔQ_S in the morning (Fig. 5) but Q_H in the afternoon. The upward spike in the χ curve at 1800 LAT is not significant, being only an artifact of ratios of small quantities near sunset. The daytime and all-day values of χ in Miami are 0.42 and 0.49, respectively, which are near the middle of the range of values observed in urban areas (Grimmond and Oke 1999a).

Turbulent latent heat flux (Q_E). The temporal form and absolute values of the ensemble-average turbulent latent heat flux (Q_E) in Miami (Fig. 6b) are similar to those observed in other North American suburban areas (Grimmond and Oke 1995). Initially this was somewhat unexpected: the presumed increased availability of heat and moisture at the surface in a subtropical city with frequent precipitation might boost evaporation. The observed pattern is a unimodal curve with its peak near midday (Fig. 6b). As at most other urbanized sites, evaporation remains positive, although small, throughout the night. Results are most similar to those for an irrigated suburb of Los Angeles (Grimmond and Oke 1995).

The overall temporal form of Y is reasonably similar to those of four other North American cities (Grimmond and Oke 1995). In all five cities Q_E is almost always positive, so Y changes sign with Q^*. Daytime values in the five cities average 0.3 ± 0.1. Unlike χ, the daily variation of Y does not show hysteresis. Through the middle eight hours of the day, Y is approximately 0.27, and for the whole day it is 0.33. Aside from the sunrise/sunset periods the standard deviation of hourly Y values exhibits very little variation throughout the daytime. In a sense this follows since the opposite trends of the two sensible heat fluxes offset each other leaving a relatively constant fraction of the net radiation for evaporation.

Descriptive parameters. Examination of the energy partitioning and controls on evaporation is aided by use of several descriptive parameters. Here we use the following:

- **Bowen's ratio** ($\beta = Q_H/Q_E$) describes the partitioning of available energy A ($= Q^* - \Delta Q_S$) between the two turbulent fluxes.
- **Priestley–Taylor aridity parameter** α_{PT} ($= Q_E/Q_{Eq}$); equilibrium evaporation Q_{Eq} is that for ex-

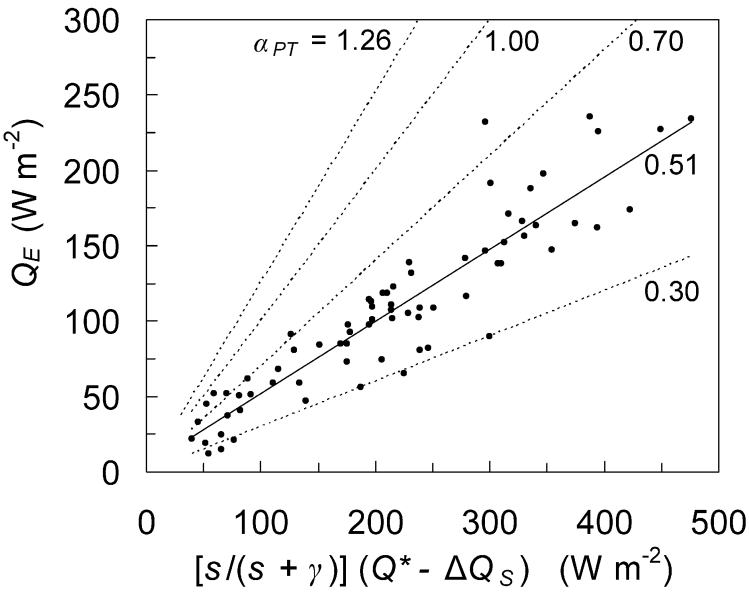

Fig. 8. Ensemble daytime ($Q^* > 0$ W m^{-2}) hourly averages of observed evaporation Q_E versus equilibrium evaporation Q_{Eq}. The slope of the solid line is the average α_{PT} for these data, i.e. 0.51

tensive surfaces with sufficient water calculated as $Q_{Eq} = [s / (s + \gamma)]\ (Q^* - \Delta Q_S)$.

– **McNaughton–Jarvis coupling factor** Ω which expresses the degree of coupling between the turbulent surface layer and the full planetary boundary layer, and takes values between zero (strongly coupled) to unity (decoupled). It is defined:

$$\Omega = [1 + \gamma\,(r_c/r_{aH})\,/\,(s + \gamma)]^{-1}$$

Here r_{aH} is taken to be 2.32 $r_{aM,}$ where r_{aM} is the aerodynamic resistance to the vertical transfer of momentum calculated from the friction velocity. r_c is obtained by rearranging Equation 4:

$$r_c = [(s\beta/\gamma) - 1]\ r_{aH} + [(\rho_a\, c_p V)/(\gamma\, Q_E)]$$

The variation of the ensemble-average β for Miami follows a fairly typical daily pattern (Fig. 7). The daytime and all-day average β values are 1.55 and 1.47, respectively. The daytime value is towards the lower end of the observed range (1.37–2.87) for suburban sites (Grimmond and Oke 1999a); however, given the wetness of the surface in west Miami a value greater than unity is a little unexpected. Nocturnal values are rather erratic because of the instability of ratios of small numbers, but it seems that values are somewhat less than the –1 commonly found in cities (Grimmond and Oke 1999a, 2002).

Observed hourly averages of α_{PT} are within the range of those from other studies (Oke *et al.* 1999). Miami daytime values mostly lie in the range 0.3 to 0.7, with an average of 0.51 (Fig. 8). This is well below the *c.*1.26 value observed for many surfaces with abundant moisture (McNaughton and Spriggs 1989). However, it is in the upper-middle portion of the observed urban range, which includes daytime averages as low as *c.* 0.35 in Tucson and during a particularly dry summer without irrigation in Vancouver, and extends as high as 0.55 in Sacramento (Oke *et al.* 1999; Grimmond and Oke 1999c). One might have expected greater values in Miami than Sacramento. But the evaporation environments of the two are quite different: rates may be stifled in Miami by the low vapour pressure deficit and enhanced in Sacramento by edge and oasis-edge effects around irrigated lawns and parks, and its high proportion of vegetated surfaces compared to most cities (Grimmond and Oke 1999a).

In many suburban and rural areas, the daily α_{PT} pattern is reasonably constant in the middle of the day, with higher values towards sunrise and sunset. The late afternoon decrease in Miami is therefore somewhat anomalous (Fig. 9a). Notice also that ß shows an unusual increase at about the same time (Fig. 7). The relatively large drop may be due to an increase in stomatal resistance r_s, with the rapidly falling light levels. Earth–Sun geometry results in very little twilight at low latitudes. Also note that α_{PT} depends on A and that in the late afternoon ΔQ_s becomes a relatively large heat source for evaporation at a time when Q^* is also positive.

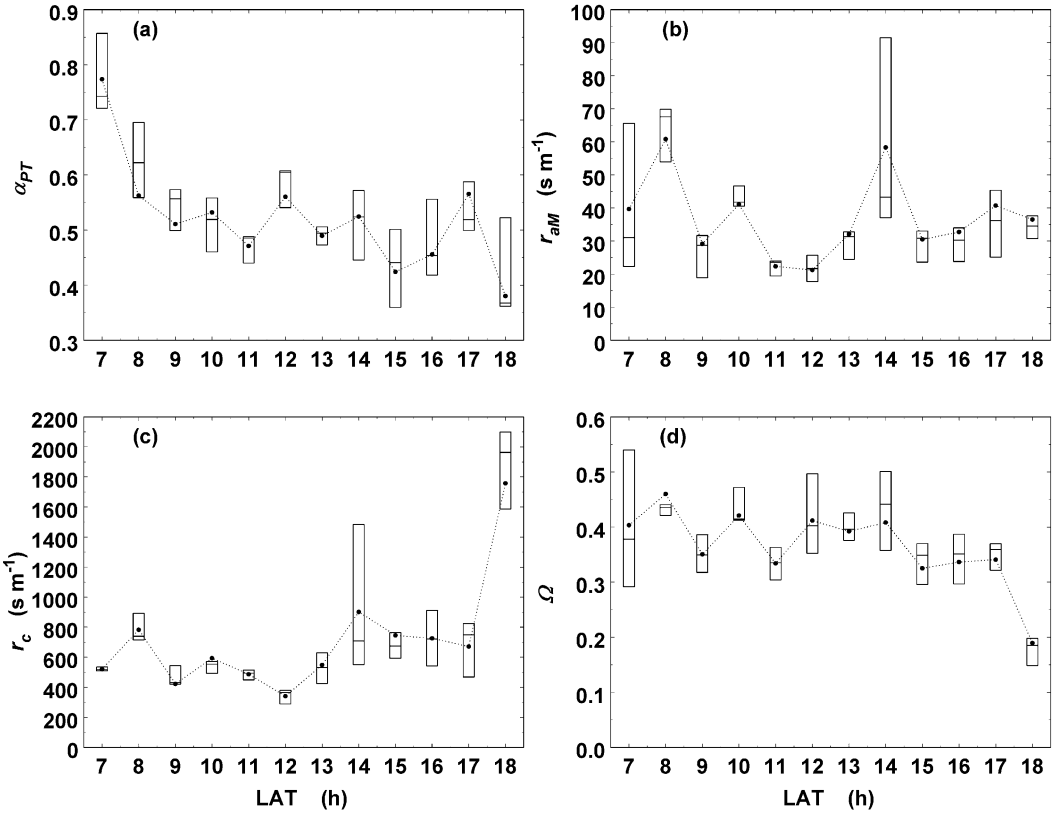

Fig. 9. Ensemble hourly averaged (a) Priestley–Taylor parameter, $\alpha_{PT,}$ (b) aerodynamic resistance to vertical transfer of horizontal momentum r_{aM}, (c) canopy resistance to vertical transfer of water vapour r_c, calculated using the Penman–Monteith equation and observed Q_E, and (d) the McNaughton–Jarvis coupling parameter Ω

Urban values of r_{aM} are usually small compared with most rural or water surfaces, due to the large roughness (Grimmond and Oke 1999b). Miami is no exception, with values typically lying between about 20 and 40 s m^{-1} with occasionally higher (lower) values due to greater (lesser) airflow (Fig. 9b).

The canopy resistance to the vertical transfer of water vapour is a significant control on evaporation, expressing as it does the role of physiologic control exerted by plant stomata. In a city this remains true, but soil and construction materials are also involved in the path between stores of water and the atmosphere. Given the lush vegetation and numerous lakes and canals, it is reasonable to presume that in Miami the resistance to water transport is relatively low by urban standards. The results show r_c about 500 s m^{-1} during the morning, 800 s m^{-1} in the evening, and jumping to *c.* 1800 s m^{-1} near sunset (Fig. 9c). These values are in the middle of the previously observed range of suburban values, and are similar to r_c observations from Vancouver (Grimmond and Oke 1991), rather than on the lower end as expected.

The average daytime Ω in Miami is about 0.4 (Fig. 9d). Ω can be as high as 0.8 for grassland and as low as 0.2 for cities (Oke 1997). Typical suburban values for Tucson are *c.* 0.1, for Vancouver between 0.1 and 0.2, and Sacramento *c.* 0.2 to 0.3. Hence the Miami values are higher than normal suggesting that its surface is somewhat more 'decoupled' from its boundary layer than most other suburban sites.

Parameterization and modelling

Very few urban areas observe radiation fluxes, especially those that involve upwelling or longwave

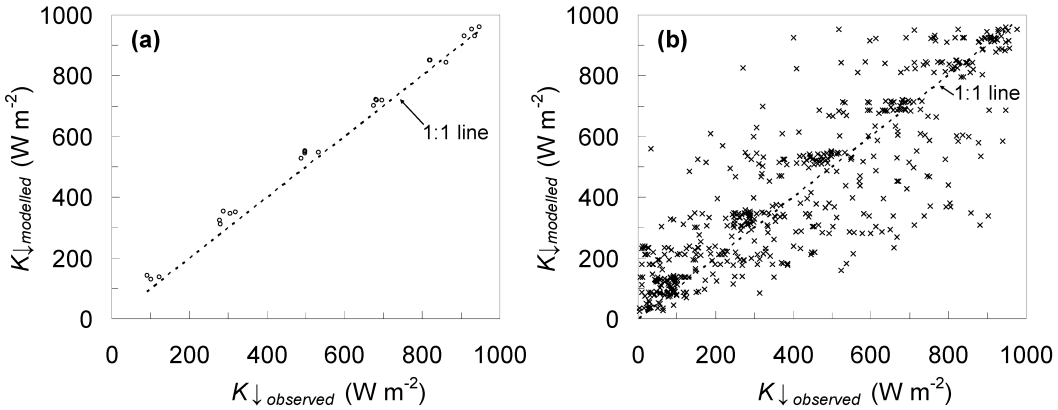

Fig. 10. $K\downarrow$ parameterized using the formula recommended by Holtslag and Van Ulden (1983) versus $K\downarrow$ observed during (a) cloudless and (b) all-sky conditions. Cloudless case statistics: $K\downarrow_{modelled} = 0.97\ (K\downarrow_{observed}) + 49.22$ W m^{-2}; MAE = 33, RMSE = 36, MBE = 31 W m^{-2}, d = 0.93, $R^2 = 0.997$, SE = 16.48 W m^{-2}. Corresponding values for all-sky case: $K\downarrow_{modelled} = 0.81\ (K\downarrow_{observed}) + 89.94$ W m^{-2}; MAE = 107, RMSE = 152, MBE = 13 W m^{-2}, d = 0.92, $R^2 = 0.727$, SE = 142.15 W m^{-2} (abbreviations are explained in Table 2 footnote)

fluxes. This is a significant deficiency especially for operational and modelling work wherein their availability could be used in a meteorological preprocessor to derive other important variables such as the turbulent sensible heat flux, or mixing height or stability. Hence it is useful to use the present observations to seek parameterizations which would only require the input of standard observations. Here we test commonly used rural parameterizations to assess their utility in both a subtropical and an urban context. The aim is only to assess the usefulness of these well known approaches in both an urban and a subtropical environment. We do not suggest or recommend that the empirical equations derived from these analyses should be used at other sites.

Solar radiation

Holtslag and Van Ulden (1983) suggest a simple approach to calculate clear-sky $K\downarrow$ which requires only the solar elevation angle (ϕ)

$$K\downarrow = a_1 \sin\phi + a_2 \qquad (5)$$

where a_1 and a_2 are empirical coefficients. The authors suggest values for a_1 ranging from 910 to 1100 W m^{-2}, and a_2 from –69 to –30 W m^{-2}. Here we use 990 and –30 W m^{-2} as suggested for temperate, mid-latitude sites by Hanna and Chang (1992). The formula works acceptably well, especially considering the coefficients used are meant for a different climatic zone (Fig. 10a). Equation 5 slightly overpredicts $K\downarrow$, perhaps due to lowered transmissivity over Miami as a result of air pollution and the subtropical marine vapour haze. Time series show the discrepancy between modelled and measured is greater in the morning than the afternoon.

Holtslag and Van Ulden (1983) also suggest a simple formula to calculate all-sky $K\downarrow$ by including fractional cloud cover N:

$$K\downarrow = (a_1 \sin\phi + a_2)(1 - b_1 N^{b2}) \qquad (6)$$

where ϕ, a_1 and a_2 are as in Equation (5), N varies from 0 (no cloud) to 1 (overcast). The b_1 and b_2 coefficients are assumed to be 0.75 and 3.4, respectively, based on observations at Hamburg, Germany, and are expected to vary with cloud type and ceiling height.

The formula does not perform well with the Miami dataset in all-sky conditions (Fig. 10b). A weakness in the present study is the fact that $K\downarrow$ was observed at the Fair site, whereas the hourly cloud fraction is from the Airport, which is 10 km distant. Given the spatial and temporal variability in cloud cover in Miami, this discrepancy must lead to degradation of performance. Altering a_1 and a_2 coefficients does not improve matters since the difficulties are clearly related to the scatter, not the slope of the relation (Fig. 10b).

Longwave radiation

Several formulae are used to calculate clear-sky $L\downarrow$ using screen-level air temperature and sometimes humidity. They are the Swinbank (1963) and Idso–

Table 2. Performance statistics for hourly incoming longwave radiation calculated from bulk formulae versus measured in Miami. Cloudless hours use original equations, all-sky hours use clear-sky equations modified by Bolz correction. Sine correction to account for daily cycle. Units of SE, MAE, MBE and RMSE are W m^{-2}

Equation	Swinbank	Idso-Jackson	Brutsaert	Satterlund	Idso	Prata
Cloudless ($L\downarrow_{clear}$) n = 95						
SE	12.91	13.66	10.04	8.88	13.25	9.57
R^2	0.32	0.32	0.52	0.47	0.47	0.52
MAE	10	14	16	15	39	14
RMSE	14	17	19	18	41	17
MBE	–2	9	15	14	39	13
D	0.76	0.70	0.68	0.67	0.40	0.71
All-sky ($L\downarrow_{all\text{-}sky}$) n = 974						
SE	19.95	20.78	18.12	18.09	20.32	17.94
R^2	0.478	0.476	0.564	0.525	0.557	0.559
MAE	17	17	18	17	41	17
RMSE	21	22	23	21	46	21
MBE	–6	6	14	11	41	12
D	0.80	0.80	0.78	0.79	0.55	0.80
Cloudless including 'sine correction'[1] n = 879						
SE	7.56	8.02	7.71	5.97	9.51	7.37
R^2	0.51	0.51	0.65	0.63	0.67	0.65
MAE	8	8	7	7	7	7
RMSE	10	10	8	9	10	8
MBE	–2	–2	0	–1	2	–1
d	0.82	0.83	0.90	0.86	0.89	0.89
[1]c_1, c_2, c_3	17.5, 1, 2	19, 1, 13	12, –2.5, 12	10.75, 0.5, 15.75	17, –5, 30	11.5, –2.5, 10.5

SE, standard error; R^2, coefficient of variation; MAE, mean absolute error; RMSE, root mean square error; MBE, mean bias error; d, Willmott index of agreement (Willmott 1984)

Jackson (1969) formulae which require only near-surface air temperature (T_a, in K) as input, plus four others by Brutsaert (1975), Satterlund (1979), Idso (1981) and Prata (1996), that also require near-surface water vapour pressure (e_a, in hPa). These are referred to here as dual-input equations. To include the presence of cloud the clear-sky equations were modified using a version of the Bolz (1949) relation:

$$L\downarrow_{cloudy} = L\downarrow_{clear}(1 + a_l N_l{}^2 + a_m((1 - N_l)N_m)^2 + a_h((1 - (N_l + (1 - N_l)N_m))N_h)^2) \quad (7)$$

where the a coefficients are 0.2275 for low, 0.185 for mid-level, and 0.06 for high cloud, N is the fractional cloud cover and the subscripts l, m and h stand for low, mid- and high level, respectively. This accounts for the influence of cloud base temperature and cloud cover (see Oke 1987) using data from Miami International Airport, located 10 km northeast of the Fair site.

All formulae provide reasonable rough estimates of Miami's clear sky $L\downarrow$ (Table 2). It is difficult to assess the best method but taken overall, of the temperature-only equations Swinbank is superior and of the dual-input equations Prata scores well. Only 95 clear-sky data points are available, a limitation which contributes to the relatively low R^2 values. The four dual-input equations over-estimate $L\downarrow_{clear}$; this may be a subtropical coastal effect because there is a sharper drop in e_a at the top of the mixing layer compared with mid-latitude layers over land. South Florida is dominated by a marine boundary layer advected from the tropical ocean. Hence the dual-input equations derived over mid-latitude areas may over-estimate the contribution of e_a to ε_a from the whole atmospheric column.

Paltridge (1970) noted a systematically varying diurnal error between Swinbank's clear-sky equation and measured values. He attributed this to the use of screen-level temperatures which over-estimate the diurnal variation of temperature in the whole atmospheric column contributing to the incoming flux at the surface. He corrected this error by adding or subtracting the appropriate amount. Here we apply a 'sine correction' calculated as:

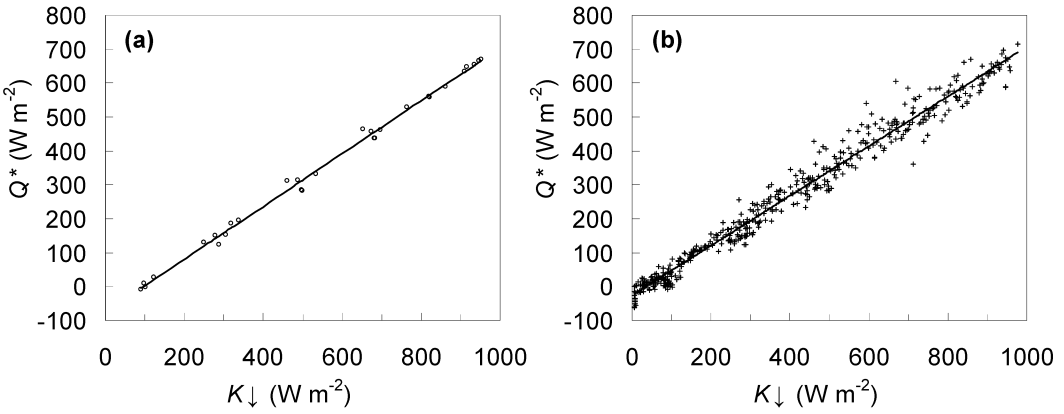

Fig. 11. Hourly averages of daytime $Q^*_{\text{residential}}$ versus $K\downarrow$, during (a) cloudless and (b) all-sky conditions. Cloudless case statistics: $Q^*_{residential} = 0.78\ (K\downarrow) - 74.86$ W m^{-2}; $R^2 = 0.996$, SE = 15.06 W m^{-2}. All-sky case statistics: $Q^*_{residential} = 0.73\ (K\downarrow) - 25.48$ W m^{-2}; $R^2 = 0.977$, SE = 31.63 W m^{-2} (abbreviations are explained in Table 2 footnote)

$$L\downarrow_{corrected} = L\downarrow_{modelled} + (c_1 \sin\{(H + c_2)(\pi / 12)\} - c_3) \quad (8)$$

where the sine function is calculated in radians, H is LAT in hours, and c_1, c_2 and c_3 are empirical constants with different values for each of the formulae (Table 2). All of the corrected formulae perform significantly better and the dual-input ones slightly outperform the single-input equations (Table 2). It may be useful to see whether the coefficients have utility at other locations.

In all-sky conditions, the standard error for each formula is approximately twice its clear-sky value (Table 2). The main reasons are probably that the cloud and radiation measurements were not co-located so the sky conditions seen by the cloud observer and the pyrgeometer were different, and the unrealistic attempt to express the complex radiative effects of cloud using only three coefficients. The Idso equation performs particularly poorly. With cloud the amplitude of the sinusoidal error is decreased relative to the clear-sky case. This is likely due to moderation by clouds of the diurnal variation of the lapse rate.

Net radiation

Over many surfaces there is a linear relation between $K\downarrow$, that is more easily measured or calculated, and Q^* that is useful in energy balance applications but is rarely available. The Miami data show a strong linear relation ($R^2 > 0.99$) in both cloudless and all-sky conditions (Fig. 11). The fit seems good at both low and high radiation loads. Even in cloudy conditions the standard error is less than 21 W m^{-2}. These results suggest there is merit in using a solarimeter to parameterize Q^* in urban areas.

For rural surfaces Holtslag and Van Ulden (1983) suggest that

$$Q^* = ((1 - \alpha)K\downarrow + d_1 T_a^{\,6} - \sigma T_a^{\,4} + d_2 N) / (1 + d_3) \quad (\text{W m}^{-2}) \quad (9)$$

requires knowledge only of α, observed or calculated $K\downarrow$, near-surface T_a, N, $d_1 = 5.31 \times 10^{-13}$ W m^{-2} K^{-6}, $d_2 = 60$ W m^{-2}, $d_3 = 0.38((1 - \alpha_{PM})S + 1) / (S + 1)$ where α_{PM} is the Penman–Monteith surface moisture availability factor and $S = c_p/(L_e \partial q_s/\partial T)$ where c_p is the specific heat of air at constant pressure, L_e is the latent heat of water vaporization, and $\partial q_s/\partial T$ is the slope of the saturation specific humidity curve. Here we use $\alpha = 0.15$ as a typical suburban value (Oke 1988); $K\downarrow$ is calculated from Equation 6; T_a and N are taken from the Miami Airport observations; $\alpha_{PM} = 1$ (Hanna and Chang 1992); and S is calculated from the airport T_a.

In clear-sky conditions the Holtslag and Van Ulden formula works well (Fig. 12a) but in all-sky conditions there is a significant increase in error. Essentially these results reflect the differing ability of Equation 6 to predict the solar input with and without cloud. Equation 6 has a standard error of 142 W m^{-2} for $K\downarrow$ under all-sky conditions which translates into an error in Q^* of about 90 W m^{-2}. There is a tendency for Equation 7 to under-estimate at values greater than 500 W m^{-2}, and to over-estimate below 100 W m^{-2}.

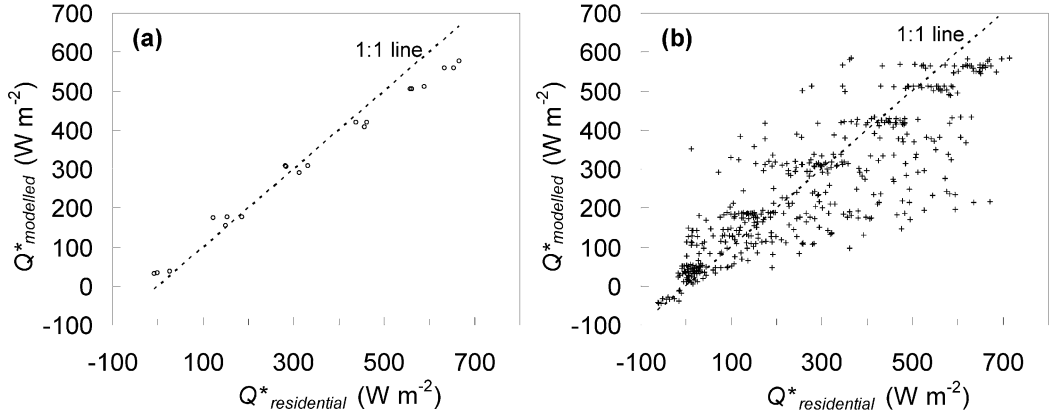

Fig. 12. Daytime Q^* parameterized using Holtslag and Van Ulden (1983) versus $Q^*_{residential}$ observations, in (a) cloudless and (b) all-sky conditions. Cloudless case statistics: $Q^*_{modelled} = 0.81\ (Q^*_{residential}) + 44.47$ W m^{-2}; MAE = 40, RMSE = 48, MBE = –20 W m^{-2}, d = 0.985, $R^2 = 0.991$, SE = 17.77 W m^{-2}. All-sky case statistics: $Q^*_{modelled} = 0.70\ (Q^*_{residential}) + 56.94$ W m^{-2}; MAE = 80, RMSE = 112, MBE = –23 W m^{-2}, d = 0.909, $R^2 = 0.722$, SE = 90.45 W m^{-2} (abbreviations are explained in Table 2 footnote)

Turbulent heat fluxes

Holtslag and van Ulden (1983) suggest a parameterization for daytime turbulent heat fluxes based on a simplified version of Penman–Monteith (Equation 4):

$$Q_H = [(1 - \alpha_{PM} + S) / (1 + S)] (Q^* - \Delta Q_S) - \beta_{PM}\ (\text{W m}^{-2}) \quad (10a)$$

$$Q_E = [\alpha_{PM} / (1 + S)]\ (Q^* - \Delta Q_S) + \beta_{PM}\ (\text{W m}^{-2}) \quad (10b)$$

Hanna and Chang (1992) recommend it for urban areas as do Grimmond and Oke (2002). Two empirical parameters are required: the Penman–Monteith surface moisture availability factor (α_{PM}), which depends on surface moisture availability, and β_{PM}, which accounts for the uncorrelated part. Here these parameters were back-calculated using the observed energy budget and linear regression of Q_H and Q_E against the available energy A to yield $\alpha_{PM} = 0.51$ and $\beta_{PM} = 2.3$.

Applying Equations 10 to the Miami suburban data yields good agreement between calculated and observed Q_H and Q_E for all-time, all-sky conditions (Fig. 13). The good result is of course not an independent test of the approach since the calculations included observed Q^*, residual ΔQ_S, and α_{PM} and β_{PM} values derived from the same observations. They are helpful, however, in demonstrating that the approach can partition the A into Q_H and Q_E with standard errors of only 17 W m^{-2}. Further, the equations appear to be equally applicable by day and night. The approach and the coefficients derived for Miami are part of the LUMPS scheme of Grimmond and Oke (2002) to estimate urban energy fluxes using only standard meteorological data and simple surface description as inputs.

Discussion

Q_E fluxes observed in Miami are lower than initially expected. Suburban sites in Los Angeles, Sacramento, Chicago and Basel have lower average Bowen ratios and a higher fraction of net radiation used in evaporation (Grimmond and Oke 1999b; Christen and Vogt 2004). Here we use the Penman–Monteith combination model (Equation 4) as a framework to discuss plausible explanations for this result.

The available energy, A, depends on both the absolute radiation input and the fraction of it sequestered in storage. The storage fraction in Miami (30%), as discussed, is relatively large and this may be part of the reason for the relatively small Q_E.

The vapour pressure deficit, V, in Miami is small (daytime about 7 to 14 hPa). If V is increased threefold (the value in Sacramento) Equation 4 suggests it boosts Q_E by about 50% of the observed flux, giving an average hourly increase of 52 W m^{-2}, or 93 W m^{-2} at noon. A six-fold increase (to the value in Tucson) raises the average hourly increase to 130 W m^{-2} and more than doubles Q_E at noon. It appears, therefore, that V can suppress Q_E. On the other hand, dividing V by three causes a drop of only about 20% in daytime Q_E because V is already low.

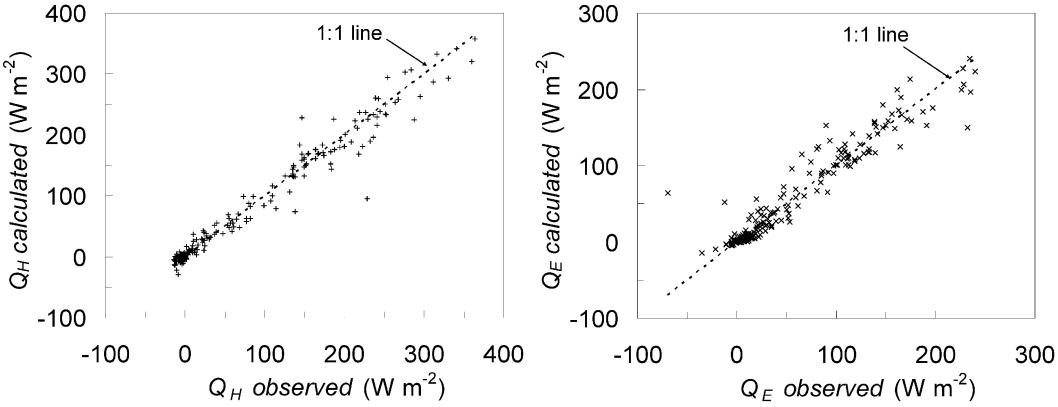

Fig. 13. Hourly averaged Q_H and Q_E calculated using Holtslag and Van Ulden (1983) versus observed fluxes in all-sky conditions. Q_H statistics: $Q_{H\ calc}$ = 0.95 ($Q_{H\ obs}$) + 2.45 W m^{-2}; MAE = 10, RMSE = 18, MBE = –1 W m^{-2}, d = 0.992, R^2 = 0.968, SE = 17.11 W m^{-2}. Q_E statistics: $Q_{E\ calc}$ = 0.94 ($Q_{E\ obs}$) + 3.70 W m^{-2}; MAE = 10, RMSE = 18, MBE = 1 W m^{-2}, d = 0.980, R^2 = 0.922, SE = 17.41 W m^{-2} (abbreviations are explained in Table 2 footnote)

The response to changes in V might be even more marked were it not for the relatively large average daytime Ω of 0.40 in Miami which signals relatively weak coupling between the surface and the deeper boundary layer.

Miami is certainly a relatively breezy city. It is true that many trees were damaged by Hurricane Hugo in 1989 but when the buildings are included the roughness length is still estimated to be 0.46 m, which keeps r_{aM} (and by extension probably r_{aH}) low, hence r_{aH} is not likely to explain the relatively low Q_E. Neither is r_c: even with about 40% of the surface covered by water or vegetation (Table 1) r_c values are similar to those of temperate suburbs. The reasons require fuller study; it seems that the mix of low open water with low resistance, vegetation of intermediate and built materials with high resistance combine to produce intermediate r_c. It is also possible that the damage caused by Hugo reduced transpiration.

Conclusions

The original motivation for the study was to investigate the anticipated differences possessed by a suburban site in a hot, wet climate compared with that of the more numerous suburban energy-balance studies in temperate climates. The outcome has been to find in the main that similarities rather than differences prevail. Thus real differences in the properties of the surface and the atmosphere seem to combine to produce radiation and energy-balance partitioning that is fairly similar to those documented for sites at higher latitudes. Further, the methods developed elsewhere seem to apply at this Miami site, in particular the following.

- The surface albedo, averaged over clear and all-sky conditions, is about 0.17, and ε_o is estimated to be 0.97.
- Measurements of Q_H, χ, Q_E, Y, ΔQ_S and Λ in Miami are similar to those from similar residential districts of other North American cities. The trends of χ and Y show remarkably little variability in the daytime, suggesting a robust basis for parameterization.
- The expectation that the Bowen ratio would be small and Q_E large relative to other cities was not observed (β is *c.* 1.5 and Y is only 0.3 and average α_{PT} is *c.* 0.51). It is thought this is due in part to relatively large storage in the wet soils, but probably mostly due to evaporation being stifled by the small vapour pressure deficit in Miami and the relatively weak surface–planetary boundary layer coupling (Ω is *c.* 0.4), suggesting A is a more significant control on evaporation than in other cities.
- Observed values of r_{aM} and r_c in Miami fall within the ranges for other suburban areas.
- With clear skies reasonable estimates of $K\downarrow$ can be obtained with **root mean square error (RMSE)** of 36 W m^{-2} using only astronomical input. Similarly $L\downarrow$ can be obtained by most bulk formulae with only near-surface humidity and/or temperature with **RMSE** of 15–20 W m^{-2}.

Performance can be improved by applying a correction for systematic diurnal under- and overestimation due to the daily variation of lapse rate giving RMSE of 8–10 W m^{-2}.
- In all-sky conditions $K\downarrow$ estimates become poor (RMSE of 152 W m^{-2}); using the Bolz cloud relation $L\downarrow$ estimates are degraded but with RMSE as small as about 5%.
- Q^* can be estimated satisfactorily from co-located observations of $K\downarrow$ or calculated from weather observations with RMSE of 48 W m^{-2} in cloud-free and 112 W m^{-2} in all-sky conditions.
- The Penman–Monteith model provides a suitable basis for predicting turbulent fluxes. Appropriate coefficients are: α_{PM} *c.* 0.50, β_{PM} *c.* 2.3.

Acknowledgements

We are grateful to the Dade County Youth Fair and Exposition authorities and the Lord family for generously permitting the installation of instruments on their properties; to Andres Soux and Mark Hubble for assistance in the field and to Dr HaPe Schmid for advice regarding source area analysis. Funding was provided by the Natural Sciences and Engineering Research Council of Canada (TO).

Trevor Newton, Levelton Consultants Ltd, Calgary, AB, Canada T2P 3E8
E-mail: trevor_canuck@yahoo.ca

Dr Tim Oke, Department of Geography, University of British Columbia, 1984 West Mall, Vancouver, BC, Canada V6T 1Z2
E-mail: toke@geog.ubc.ca

Dr Sue Grimmond, Department of Geography, King's College London, Strand, London, WC2R 2LS, UK
E-mail: sue.grimmond@kcl.ac.uk

Dr Matthias Roth, Department of Geography, National University of Singapore, 1 Arts Link, Kent Ridge, Singapore 117570
E-mail: geomr@nus.edu.sg

References

Bailey, W.G., Oke, T.R. and Rouse, W.R., 2000: The Surface Climates of Canada. McGill-Queen's Press. Montréal. 369 p.

Barradas, V.L, Tejeda-Martinez, A. and Jauregui, E., 1999: Energy balance measurements in a suburban vegetated area in Mexico City. *Atmospheric Environment*, 33: 4109–4113.

Bolz, H.M., 1949: Die Abhängigkeit der infraroten Gegenstrahlung von der Bewölkung. *Meteorologische Zeitschrift*, 7.

Brutsaert, W., 1975: On a derivable formula for long-wave radiation from clear skies. *Water Resources Research*, 11: 742–744.

Christen, A. and Vogt, R., 2004: Energy and radiation balance of a central European city. *International Journal of Climatology*, 24: 1395–1421.

Davies, J.A., and Idso, S.B., 1979: Estimating the surface radiation balance and its components. *In*: Barfield, B.J. and Gerber, J.F. (eds): Modification of the Aerial Environment of Crops. American Society of Agricultural Engineers. Michigan. 183–210.

Garcia-Cueto R, Jauregui, E. and Tejeda, A., 2003: Urban/rural energy balance observations in a desert city in northern Mexico. Proceedings Fifth International Conference on Urban Climate, ICUC-5, 1–5 Sept. 2003, Lodz, Poland (Proceedings CD-ROM).

Grimmond, C.S.B. and Oke, T.R., 1991: An evapotranspiration-interception model for urban areas. *Water Resources Research*, 27: 1739–1755.

Grimmond, C.S.B. and Oke, T.R., 1995: Comparison of heat fluxes from summertime observations in the suburbs of four North American cities. *Journal of Applied Meteorology*, 34: 873–889.

Grimmond, C.S.B. and Oke, T.R., 1999a: Heat storage in urban areas: Local-scale observations and the evaluation of a simple model. *Journal of Applied Meteorology*, 38: 922–940.

Grimmond, C.S.B. and Oke, T.R., 1999b: Aerodynamic properties of urban areas derived from analysis of urban form. *Journal of Applied Meteorology*, 38: 1262–1292.

Grimmond, C.S.B. and Oke, T.R., 1999c: Rates of evaporation in urban areas. Impacts of Urban Growth on Surface and Ground Waters. *International Association of Hydrological Science Publications*, 259: 235–243.

Grimmond, C.S.B. and Oke, T.R., 2002: Turbulent fluxes in urban areas:observations and a local-scale urban meteorological parameterization scheme (LUMPS). *Journal of Applied Meteorology*, 41: 792–810.

Hanna, S.R. and Chang, J.C., 1992: Boundary-layer parameterizations for applied dispersion modeling over urban areas. *Boundary-Layer Meteorology*, 58: 229–259.

Holtslag, A.A.M. and Van Ulden, A.P., 1983: A simple scheme for daytime estimates of the surface fluxes from routine weather data. *Journal of Applied Meteorology*, 22: 517–529.

Idso, S.B., 1981: A set of equations from full spectrum and 8 to 14 μm and 10.5 to 12.5μm thermal radiation from clear skies. *Water Resources Research*, 17: 295–304.

Idso, S.B. and Jackson, R.D., 1969: Thermal radiation from the atmosphere. *Journal of Geophysical Research*, 74: 5397–5403.

McNaughton, K.G. and Spriggs, T.W., 1989: An evaluation of the Priestley and Taylor equation and the complementary relationship using results from a mixed-layer model of the convective boundary layer. *In:* Estimation of Areal Evapotranspiration. Black, T.A. Spittlehouse, D.L. Novak, M.D. and Price, D.T. (eds): IAHS Publication No. 177. 89–104.

Monteith, J.L. and Unsworth, M.H., 1990: Principles of Environmental Physics (2nd edn) Arnold. London. 291 p.

Offerle, B., Jonsson, P., Eliasson, I. and Grimmond, C.S.B., 2005: Urban modification of the surface energy balance in the West African Sahel: Ouagadougou, Burkina Faso. *Journal of Climate*, 18: 3983–3995.

Offerle, B., Grimmond, C.S.B., Fortuniak, K. , Klysik , K. and Oke, T.R., 2006: Temporal variations in heat fluxes over a central European city centre. *Theoretical and Applied Climatology*, 84: 103–115.

Oke, T.R., 1987: Boundary Layer Climates (2nd edn) Routledge. London. 435 p.

Oke, T. R., 1988: The urban energy balance. *Progress in Physical Geography*, 12: 471–508.

Oke, T.R., 1997: Urban environments. The Surface Climates of Canada. *In*: Bailey, W.G., Oke, T.R. and Rouse, W.R. (eds): McGill-Queen's Press. Montréal. (369 p) 303–327.

Oke, T.R., 2004: Initial guidance to obtain representative meteorological observations at urban sites. IOM Report No. 81. WMO/TD No. 1250. World Meteorological Organization Geneva. 51 p. website: http://www.wmo.int/web/www/IMOP/publications/IOM-81/IOM-81-UrbanMetObs.pdf

Oke, T.R., Zeuner, G. and Jauregui, E., 1992: The surface energy balance in Mexico City. *Atmospheric Environment*, 26B: 433–444.

Oke, T.R., Spronken-Smith, R.A., Jauregui, E. and Grimmond, C.S.B., 1999: The energy balance of central Mexico City during the dry season. *Atmospheric Environment*, 33: 3919–3930.

Paltridge, G.W., 1970: Day-time long-wave radiation from the sky. *Quarterly Journal of the Royal Meteorological Society*, 96: 645–653.

Prata, A.J., 1996: A new long-wave formula for estimating downward clear-sky radiation at the surface. *Quarterly Journal of the Royal Meteorological Society*, 122: 1127–1151.

Roberts, S.M., Oke, T.R. , Grimmond, C.S.B. and Voogt, J.A., 2006: Comparison of four methods to estimate urban heat storage. *Journal of Applied Meteorology and Climatology*, 45: 1766–1781.

Rouse, W.R. and Bello, R.L., 1979: Shortwave radiation balance in an urban aerosol layer. *Atmosphere-Ocean*, 17:157–168.

Sailor, D.J. and Lu, L., 2004: A top-down methodology for developing diurnal and seasonal anthropogenic heating profiles for urban areas. *Atmospheric Environment*, 38: 2737–2748.

Satterlund, D.R., 1979: An improved equation for estimating long-wave radiation from the atmosphere. *Water Resources Research*, 15: 1649–1650.

Schmid, H.-P., 1994: Source areas for scalars and scalar fluxes. *Boundary-Layer Meteorology*, 67: 293–318.

Schmid, H.-P., Cleugh, H.A., Grimmond, C.S.B. and Oke, T.R., 1991: Spatial variability of energy fluxes in suburban terrain. *Boundary-Layer Meteorology*, 54: 249–276.

Steyn, D.G. and Oke, T.R., 1980: Effects of a small scrub fire on the surface radiation budget. *Weather*, 35: 212–215.

Swinbank, W.C., 1963: Long-wave radiation from clear skies. *Quarterly Journal of the Royal Meteorological Society*, 89: 339–348.

Tanner, B.D. and Greene, J.P., 1989: Measurements of sensible heat and water vapor fluxes using the eddy correlation method. Final Report to US Army Dugway Proving Gounds. 98 p.

Tejeda-Martinez, A. and Jauregui, E., 2005: Surface energy balance measurements in the Mexico City region. *Atmosfera*, 18: 1–23.

Webb, E.K., Pearman, G.I. and Leuning, R., 1980: Correction of flux measurements for density effects due to heat and water vapour transfer. *Quarterly Journal of the Royal Meteorological Society*, 106: 85–100.

Willmott, C.J., 1982: Some comments on the evaluation of model performance. *Bulletin of American Meteorological Society,* 63: 1309–1313.

Manuscript received Feb. 2007, revised and accepted May 2007.